DEVELOPMENT OF A PERISTALTICALLY ACTUATED DEVICE FOR THE MINIMAL INVASIVE SURGERY WITH A HAPTIC SENSOR ARRAY

Authors: Johannes Dietrich, Siegfried Oberthür, Roman Preuß, Danja Voges and Petra Meier

Institution: Technical University Ilmenau, Faculty of Mechanical Engineering,
Institute of Microsystems Technology, Mechatronics and Mechanics
PO 100565 – 98684 Ilmenau, Germany
e-mail: pademis@tu-ilmenau.de

Abstract

The development of an actively moving device for minimal invasive spine surgery is introduced. Compared to commercially available endoscopes the device moves self actuated by peristaltic locomotion analogous to an earthworm and it is entirely compliant. The primary application is the endoscopic surgical treatment of herniated discs. The device is hollow inside to provide space for the insertion of endoscopic instruments. Essential procedures of the endeavour, i.e. examining the spinal canal, studying options of locomotion, testing and describing the silicon rubber material utilised, Finite Element simulation of the design, constructing a prototype facility and control unit, are represented in detail. In addition, the perspective to integrate a haptic sensor array is discussed.

Keywords: peristaltic, spinal canal, prolapse, silicone, haptic, hydraulic actuation, hyper elasticity, modal analysis

1. Introduction

In Germany, about 60.000 surgical treatments of disc prolapses take place annually [1]. There are a variety of symptoms ranging from tingling, numbness, weakness, severe pain and paralysis.

Disc prolapses are typically caused by degenerative deformation of the Nucleus pulposus inside the intervertebral disc. When the jelly-like core of the disc squeezes through the disc it may expand inside the spinal canal and might irritate and compress the nerves of the spinal cord. About 90% of prolapses are occurring within the lumbar region, 9% are observed within the cervical region, and the remaining 1% within the thoracal region of the spinal column.

When non-operative treatments have failed a portion of the herniated disc that is causing the nerve compression is surgically removed. In contrast to conventional surgery, which requires large open incisions and extensive muscle dissections the development of optical endoscopes and special instruments has made it possible to perform minimal invasive spine surgery. Here the surgeon is placing rigid trocars that are used for guidance of optics and manipulation tools towards the prolapse. In most cases, the muscles are pushed aside rather than being cut, but in either case a muscular trauma occurs. Moreover, in order to get inside the spinal canal it is drilled through a vertebrae or disc. Once the instruments are inserted towards a specific location they cannot be rerouted. In order to achieve a different location new incisions are necessary. With this restricted manoeuvrability it is not possible to approach more than one disc for diagnosis or further surgical treatments. Furthermore, there is a high probability that small muscles supporting the vertebral bodies are being irreversibly destroyed.

These disadvantages of the standard Endoscopic discectomy encouraged the launch of a research project developing a **P**eristaltically **A**ctuated **De**vice for **M**inimal **I**nvasive **S**urgery (PADeMIS), whose primary application is the minimal invasive spine surgical treatment of herniated discs.

Surgery will be performed in an open MRI for monitoring, navigation and safety reasons. The device is entering the spinal canal at the os sacrum and is progressing cranially between the vertebral bodies and the Dura mater spinalis as shown in Figure 1.1.

Figure 1.1: Path of PADeMIS

Due to the irregular sized pathway (diameter ranging from 4mm to 10mm) and the highly sensitive environment as described in chapter 2 and because of the radiated magnetic field the device is entirely going to be made of a soft, non-metallic and flexible material that is permitted for medical use. The principles of locomotion are demonstrated in chapter 3. Material options are discussed further in section 4.1. In order for the surgeon to insert endoscopic instruments the device must be hollow inside and be connected to a hollow tube that is leading to the outside of the patient. The design and possibilities to manufacture such a device are outlined in chapters 4 and 5.

For diagnostic support a method that measures quantities of tactile sense in-vivo and outputs them visually or stimulant to the surgeon are investigated and first approaches displayed in chapter 6.

2. Environmental conditions

The spinal canal is essentially a tunnel that runs down the entire length of the spine from the skull to the sacrum. It is encircled by the vertebral bodies forming the spine and it contains the spinal cord, which is an elemental part of the central nerve system and branches of in nerve roots in the lumbar region.

2.1. Anatomical layout of the spinal canal

In an adult the spinal cord extends from the top of the Atlas (first vertebrae, C1) to the lower border of the first lumbar vertebra. There it divides into a bundle of many different nerve roots, which are named Cauda equina. The spinal cord is protected by a rather stiff dural sheet, called Dura mater spinalis (thickness ~2mm). The space between the dura and the vertebral bodies is called epidural space. It contains ligaments (Ligamenta flava, Ligamentum longitudinale posterius) and is filled with fat tissue and Plexus venosus internus that provides the venous drainage for the individual vertebral body. The available minimum working space of the device being developed inside the epidural space is limited to a diameter of 4mm and may vary up to 10mm. [2-4].

2.2. Resistance-force Measurements

The force required for the forward motion of the device was estimated experimentally on just euthanised pigs. A Fogarty catheter was entered from dorsal into the lumbar region of the spinal canal between L4 and L5. The catheter was equipped with a force sensor. After the force required to insert the catheter cranially towards the cervical region was recorded the balloon at the front of the catheter was inflated. The force needed to remove the catheter was measured with respect to position and size of the balloon. The experiment was conducted on 8 animals weighting 27-30kg. It was found that a minimum force of 2.6N to 4.1N is necessary to move a device of 4mm in diameter. Through those experiments it has been shown that the space available is sufficient for such a device travelling inside the spinal canal along the Dura mater. Because the experiments have been carried out on dead pigs it must

be realised that the material properties of a dead are not identical to a living animal and secondly the vertebral column of a pig is geometrically not identical to the human spine, which contains a distinctive curvature.

3. Locomotion

The device is travelling by peristaltic means like the crawling motion of an earthworm. Technically, the spinal canal is a pipe filled with semifluid tissue particles, the device must crawl past and through. Because of the natural continuous path of the canal the device progresses towards the least resistant. Although, no complex control is necessary, an option for steering to support the generally given direction is considered.

3.1. Biological Inspiration

The earthworm (Annelida: Oligochaeta) moves by peristaltic locomotion. Waves of contraction and relaxation of antagonistic muscle groups (longitudinal and circular muscles) causes the worm to move forward. Four pairs of bristles at each segment can be elevated for anchor the temporary immobile segments. The body cavity is fluid-filled and partitioned into numerous separate segments. The hydrostatic skeleton counteracts the muscle contraction.

3.2. Schematics

The locomotion is based on a propagating wave on the surface of the moving device. Technologically, a segmentation of the body is useful. The simplest functional unit for a peristaltic moving device is a structure of 3 segments - each segment allowing thickening and lengthening at the same time. Also, any other unit of more than 3 elements is possible. In fact, a serial arrangement of these kinds of units are conceivable. In peristaltic locomotion a 'step' of an unit of n elements is achieved by n switching operations. At least 2 elements of the functional unit are controlled simultaneously. The step

length is defined as the length difference between an inflated and deflated element multiplied by the number of deflated elements in the functional unit.

The length of the functional can be changed. A structure with e.g. 18 elements may be controlled by functional units of length 3, 6, 9 or 18. For PADeMIS a sequence of 6 elements is considered due to the larger step size of one cycle as shown in Figure 3.2.1. In order to provide sufficient dynamic stability during locomotion, i.e. adequate contact to the surroundings, the sequence can repeated several times.
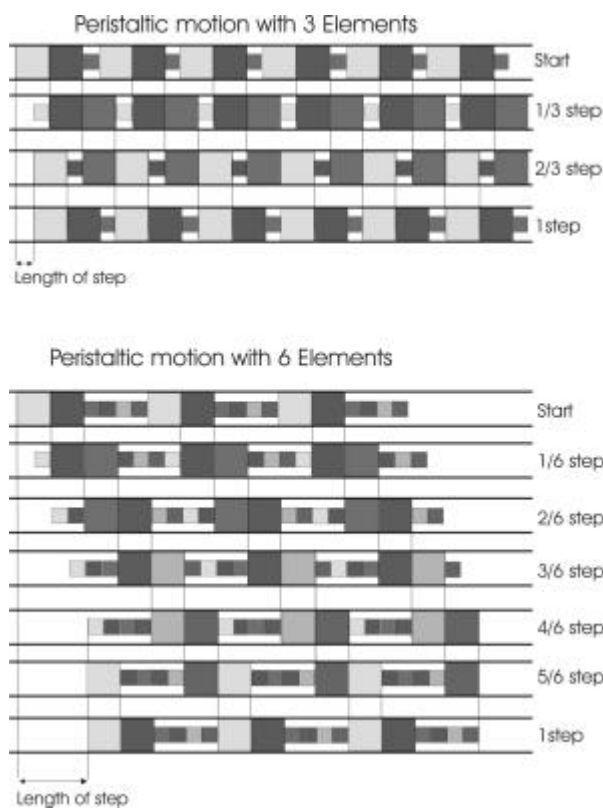

Figure 3.2.1: Schematics of peristaltic motion.

The layout of the segments are described in section 4.2. The principle of the peristaltic locomotion has been confirmed by a macro model that is described in section 5.1.

4. Design, Simulations and Actuation of PADeMIS segments

The environmental conditions explained above and the medical application restrict the choice of the material enormously. In addition, the controlled deformation and stretching of individual segment are difficult to achieve and require a precise hydraulic actuation.

4.1. Material choice

Due to the dimensions of the vertebral canal the material chosen must be hyper elastic in order to enable a variation of the device's outer diameter between 4mm and 10mm. Furthermore, the material is required to be sterilizable and it is permitted for medical use.

The large reversible stretches can be performed by rubber or rubber like materials. For natural rubber (latex) allergic reactions are being increasingly recognised. Nevertheless, silicone rubber (SR) has been a common material for medical applications. Different shore hardness can be obtained with silica filler. The SR MED49xx from Nusil is chosen for PADeMIS, where xx indicates the shore hardness. Figure 4.1.1 shows the stress-stretch relation for MED 4950 in uniaxial tension. The material shows the Mullins effect, i.e. a pre-stretched sample memorises its history [5, 6]. A recovering of the preconditioning could not be observed in a time period of 4 weeks. Therefore, a pre-stretched material is going to be used for PADeMIS. The (pre-stretched) silicone rubber shows a hyperelastic constitutive law that can be fitted by the Mooney-Rivlin law [7]. The computed parameters are used as input quantities for the simulation of the deformation of one individual segment.
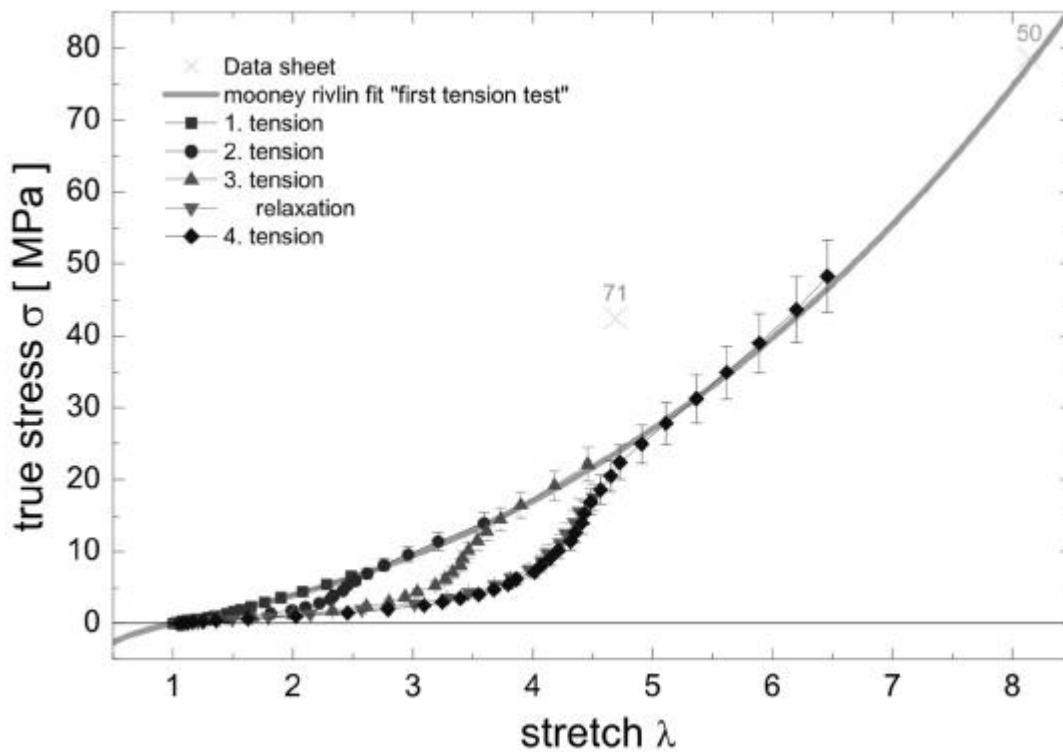
Figure 4.1.1: Uniaxial tension test of a silicone rubber sample with shore hardness 50. The material shows the Mullins effect.

4.2. Segment deformation

The peristaltic locomotion requires a segment to expand in diameter and to increase in length in the axial direction simultaneously during hydraulic filling. What is more, PADeMIS should be steerable. Therefore, the deformation should allow an axial asymmetry. While the segments are hydraulically filled and deformed the diameter of the internal hollow tunnel of the device must be maintained at 2mm.

For the design and evaluation process the Finite element software ANSYS[®] is used. The deformation of the silicone rubber is simulated with the Hyper58 element in a nonlinear calculation.

Figure 4.2.1 shows a segment of PADeMIS containing 4 cushions simulated with the material properties fitted from the uniaxial tension test of pre-stretched Nusil Med 4950. In this simulation the segment is deformed by nearly obeying the conditions stated above.
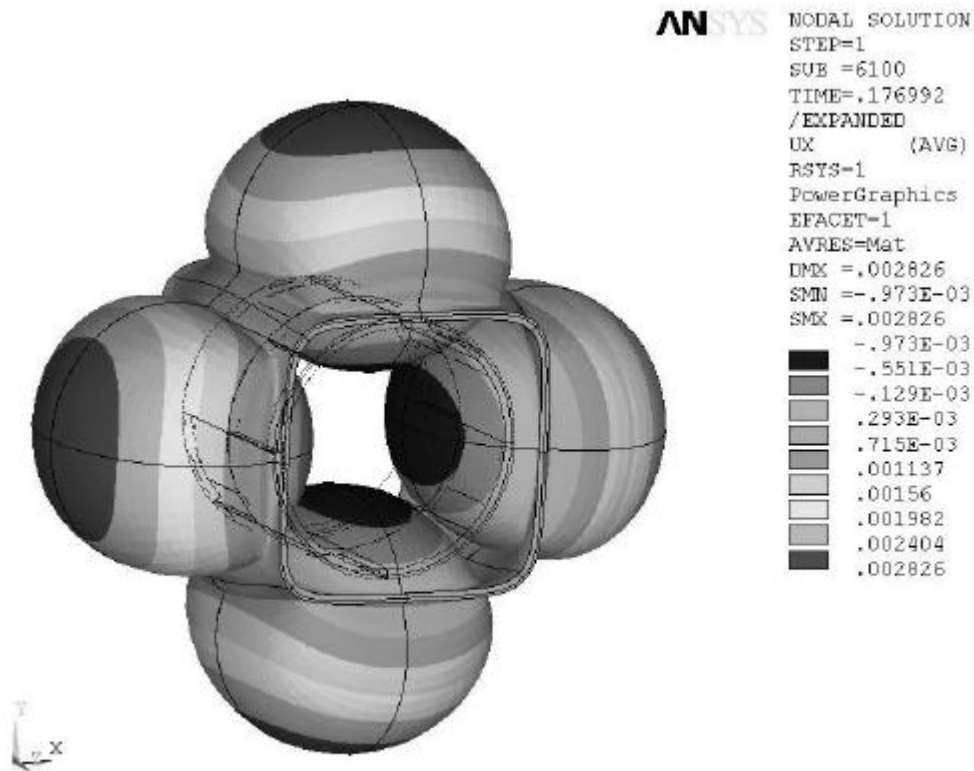

Figure 4.2.1: Radial Translation of the silicone sheets of one PADeMIS segment at pressure p=0.177bar.

Figure 4.2.2 shows the length normalised against the initial cushion length and the inner and outer diameter with respect to the pressure applied. The decrease in length at small pressures is due to the deformation of the cushion and the length increases when the SR starts stretching. Hence, this segment could be used in a tube with a minimum diameter of 5mm. The segment deformation is still being optimised.

The largest stretches in the segment occur at equibiaxial stress conditions. So far uniaxial tension tests are performed in order to calculate Mooney-Rivlin parameters. The occurring errors are difficult to estimate. Therefore, equibiaxial stress tests are necessary.
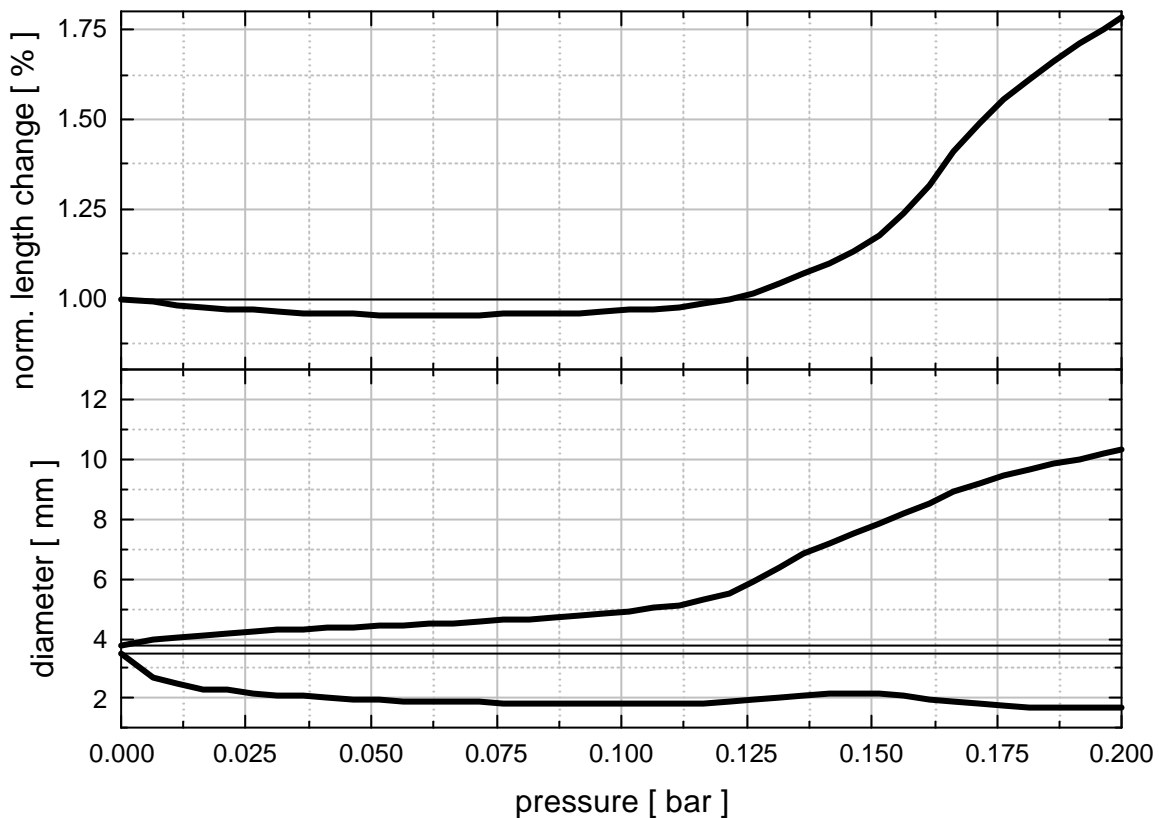
Figure 4.2.2: Pressure dependency of the inner and outer diameters and norm. length change of a PADeMIS segment.

4.3. Hydraulic control

Due to the small dimensions of the device the energy source and the control logic are coercively placed outside. The energy transmission is based on hydraulics. The current design consists of 6 sequential connected segments with four cushions each requiring 24 independently controllable hydraulic actions. Therefore a special capillary design consisting of 24 equal inlet holes and one primary hole for endoscopic tools in the middle is intended. In order to achieve the required dimensions the cross section area of one inlet hole is constrained by 100μm.

According to the simulations a deformation is achieved by filling 12 mm^3 to 32 mm^3 saline solution at 2 bars into each pillow. Because of the constrained diameter of the inlet holes the fluid resistance is reasonable large and the fluid transport rather time consuming.

10

The hydraulic actuation is achieved by a sequence of hydraulic micro pumps as shown in Figure 4.3.1. In this set-up, a servo motion is transmitted into a linear translation that drives a piston. The piston diameter is 1.5mm and the possible displacement 20 mm. The hydraulic actuation and segment deformation is achieved volume controlled with a resolution of $1\,mm^3$. The sequence and rate at which the pillows are actuated depend on the direction, velocity and steering.
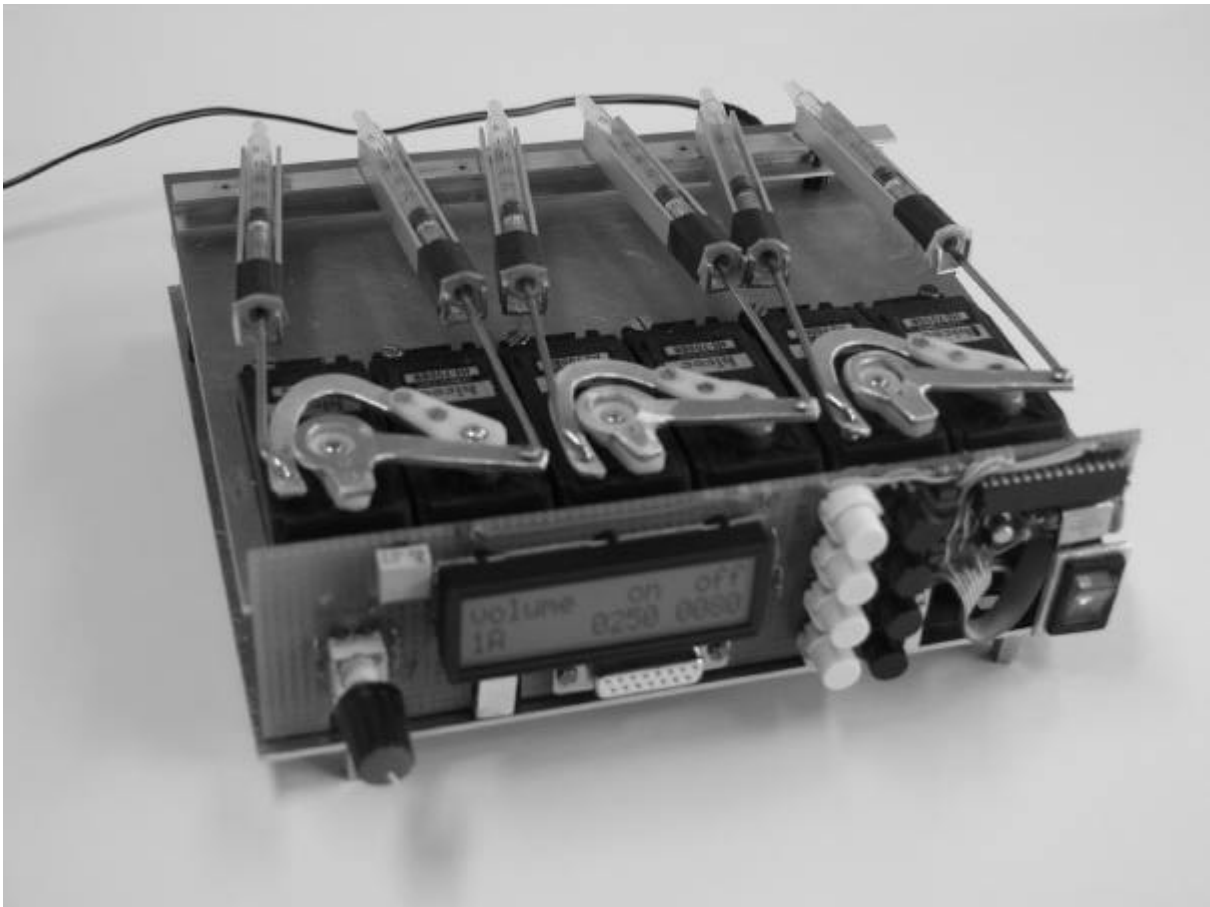

Figure 4.3.1: Micro pumps driven by stepper motors.

5. Manufacturing technology

Several conventional manufacturing technologies producing work pieces from silicone rubber have been established, e.g. injection moulding of medical implants and extrusion of infusion or transfusion tubes. In fact, most of the commercially available medical devices are produced by those techniques. Thus, more complex structures are composed of several moulded primitives. Due to the severe requirements concerning precision and complexity of the stipulated design (i.e. a cylindrical body measuring an outer diameter of 4mm, a remaining inside space of 2.5mm and an arrangement of cushions and inlet capillaries embedded into the cylindrical shell) the standard manufacturing techniques utilizing mould cores or extrusion cannot be applied to fabricate PADeMIS.

Furthermore, silicone rubber being a soft, compliant and hyper elastic material handling, positioning, gluing and post assembling are infeasible. In fact, mould cores would most certainly break during positioning, fixation or injection of LR silicone on account of their instability due to their miniature dimensions and could not be removed mechanically.

Therefore, a chemically solvable mould core material in combination with dip coating is examined. One or more sacrificial mould cores are dip-coated into a silicone solution and the silicone layers are annealed. Thereafter, the mould core is completely removed by solving it in an organic solvent. Through this technique it is intended to reduce the mechanical strain to the mould core and the silicone workpiece. [8-9].

5.1. Manufacturing and testing in macro-scale

For studying the feasibility of the manufacturing process a macro size model that is shown in Figure 5.1.1 has been produced by dip-coating and its functionality successfully examined.

The mould cores were manufactured by injection moulding. A wax-like substance that is solvable in citric acid was chosen as mould core material. The single mould cores were dip-coated into a silicone – toluene solution

(30% Elastosil™ LR3003/30). The dip-coated mould cores are inchoately annealed at a temperature below the melting point of the wax (333°K). After silicone tubes are connected to each silicone - layered mould core the individual mould cores are catenated consecutively by silicone glue. Finally, the wax is solved by citric acid and the macro-scale device connected to a pneumatic power and control system.
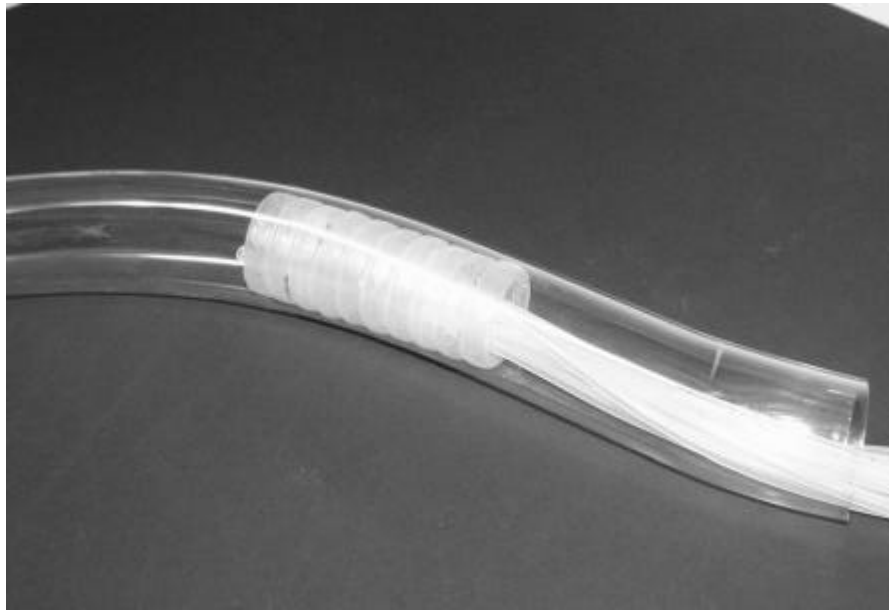

Figure 5.1.1: Peristaltically pneumatically actuated device in macro scale

5.2. Prototyping system assembly of the micro-scale device

At first, micro injection moulding with solvable, sacrificial mould cores was discovered at RWTH Aachen [10]. The sacrificial mould cores are manufactured by microinjection moulding with polycarbonate (PC). Subsequently, the micro devices, i.e. micro-venturi-nozzles, are micro moulded with polyoxymethylene (POM). Finally, PC is solved in tetrahydrofuran (THF).

The complex arrangement of the placeholders structures, which form the cushions and inlet capillaries embedded into the cylindrical shell can not be trivially manufactured by injection moulding. In addition, the wide varying ratio of length per thickness of the chamber-capillary-system (approximately

50..1000) results in an instability of the mould cores and complicates their handling.

Therefore, dip coating combined with a lithography process has been evaluated for processing silicone. Thus, PADeMIS is structured layer by layer. Hence, direct mechanical handling of the sensitive mould cores is avoided. The process sequence is displayed in Figure 5.2.1.

The cylindrical format of the device is achieved by using a cylindrical rod as substrate that is coated by a seceding film to enable the separation of the finished device from the cylindrical rod. The substrate is dip-coated by LR silicone and annealed. The sacrificial placeholder structures are attained by a layer of resist that is homogenously sprayed onto the silicone surface by an airbrush system. The resist layer is structured by laser-lithography. Thus, cushions and capillaries are formed by the remained parts of the resist. If another layer of silicone is brought onto the silicone–resist–pattern the resist regions are embedded within a silicone shell. After the silicon is annealed the resist parts are removed with acetone or another remover solution.
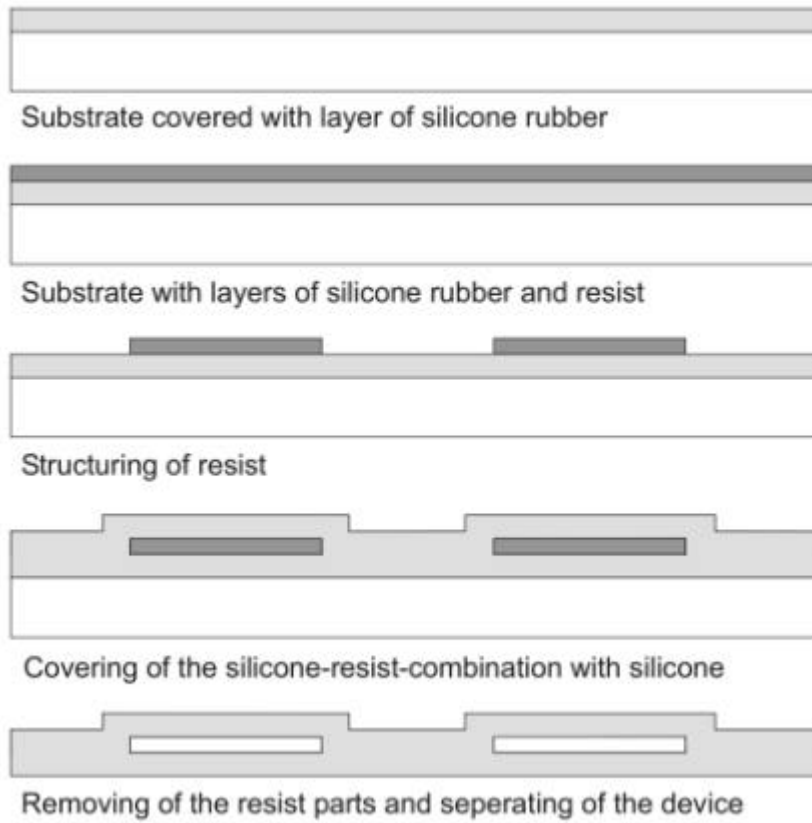
Substrate covered with layer of silicone rubber

Substrate with layers of silicone rubber and resist

Structuring of resist

Covering of the silicone-resist-combination with silicone

Removing of the resist parts and seperating of the device

Figure 5.2.1: Production process sequence

6. Haptics

In minimal invasive surgery surgeons may compensate their lack of visibility with the use of optical endoscopes, real time MRI or other image guided systems. Although endoscopic tools with force feedback do exist the sense of feel and touch as established in conventional surgery are not habitually available during endoscopic surgery [11]. For PADeMIS it is considered to integrate a component that is able to inspect the surrounding tissue in terms of its structure and material composition. It is intended to analyse data that reflects tactile sensation. Thus, a haptic sensor array is being developed and measurement and evaluation principles are examined.

Principally, biological haptics refers to the modality of touch via skin exteroceptors in combination with force proprioceptors. An observer senses the shape, texture and to a certain extend the composition underneath the surface of an object.

Three major research trends may be associated with haptics:

- Measuring tactile perception in terms of elasticity, viscosity, surface friction, temperature, etc.

- Applying findings from physiological studies of human tactile perception to the design of devices that replicate and stimulate the tactile sense and are used as output devices, e.g. finger pad, glove.

- Determining the behaviour and response of objects subject to displacement, manipulation and deformation. These are integrated into virtual environments and simulators equipped with tactile or force feedback devices, e.g. KISMET [12].

Here, the potentials of a novel method of diagnostics are studied by means of in-vivo measurements of geometrical and mechanical properties. This haptic information may be transferred from the place of surgery to an output device accessible to the surgeon. The output can be in a graphical appearance or an instrument stimulating the tactile senses in the surgeon's finger tip. The

identification of the type and state of tissue is based of the varying different mechanical characteristics, i.e. elasticity and viscosity.

6.1. Measuring Principle

The measuring principle currently observed is based on modal analysis. Modal analysis is a process, where the structure examined is described in terms of its natural dynamical characteristics (modal parameters), which are its natural frequencies, stiffness, damping and mode shapes. A test pin equipped with an impedance head (accelerometer plus force sensor) is excited by a sinusoidal signal with continuously varying frequencies (sweep) through the range of 5Hz to 150Hz. The test pin is pressed to the tissue surface structure and the input force and its response (acceleration) is recorded. The set-up can be seen in Figure 6.1.1.
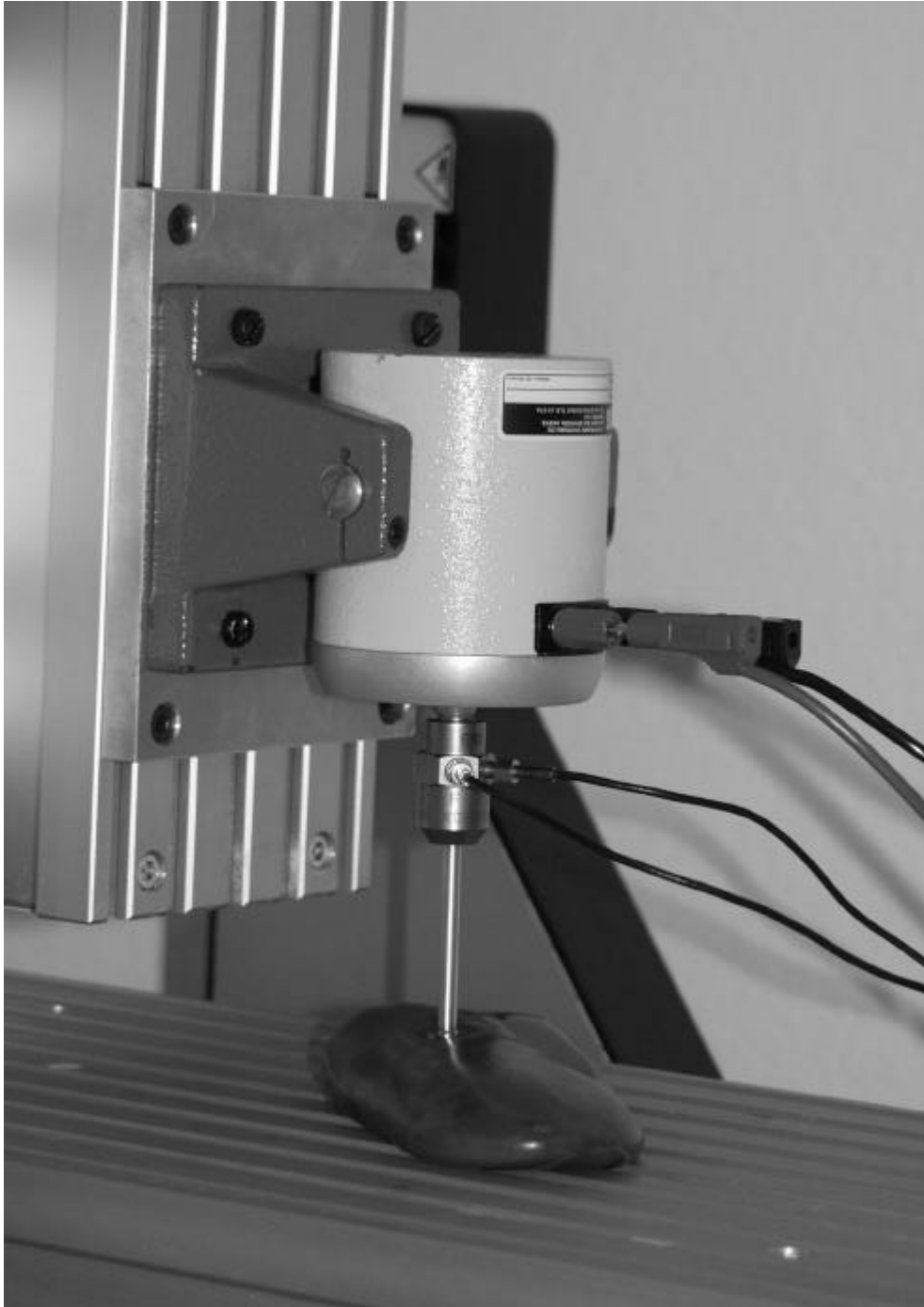
Figure 6.1.1: Apparatus measuring the modal characteristics of kidney.

For analysis, the input and the response signals are transformed into the frequency domain by applying Fast Fourier Transformation and the frequency response function is computed [13].

It can be observed, that the magnitude of the frequency response function changes depending on the rate of oscillation of the input force. It increases when the input force oscillates at a frequency that approaches one of the

natural frequencies of the excited tissue and is reaching its maximum at resonance frequency.

6.2. Identification methods

The excited tissue region may be regarded as a one degree of freedom mass-spring-damper system. Thus, the differential equation of motion is of the form:

$$m\ddot{x}(t) + c\dot{x}(t) + kx = f(t) \tag{6.2.1}$$

Here, x, $\dot{x}$ and $\ddot{x}$ are the displacement, velocity and acceleration of the mass m, k the stiffness and c the damping constant of the system (i.e. apparatus and specimen) and $f(t)$ the excitation force. A solution of the form $x(t) = Xe^{jwt}$ is assumed. w is called the circular frequency $w = 2pf$. The equation can be rewritten in the form:

$$(-mw^2 + iwc + k)Xe^{jwt} = F_0 e^{jwt} \tag{6.2.2}$$

In view of the fact that $\ddot{x} = -w^2 Xe^{jwt} = Ae^{jwt}$ the accelerance function of the system may be determined by

$$H_{\text{Accelerance}}(jw) = \frac{A(jw)}{F(jw)} = \frac{-w^2}{-mw^2 + jwc + k} \tag{6.2.3}$$

The accelerance is one option of describe the transfer function of the system and it is defined as the ratio of acceleration (output) to force (input) in the frequency domain [14]. By multiplying the equation by its complex conjugate and given that $m = \dfrac{k}{w_n^2}$, where w_n is the natural frequency of the undamped system the modulus of the accelerance function is computed as

$$\left| H_{\text{Accelerance}}(jw) \right| = \sqrt{\frac{1}{k^2\left(\dfrac{1}{w_n^2} - \dfrac{1}{w^2}\right)^2 + \dfrac{c^2}{w^2}}} \tag{6.2.4}$$

When the independent variable w approaches infinity the equation can be reduced to

$$\left| H_{\text{Accelerance}}(jw) \right|_{\lim w \to \infty} = \frac{w_n^2}{k} = \frac{1}{m_{ap} + m_{ex}}$$

19

m_{ap} and m_{ex} indicate the mass of the apparatus and the tissue being excited respectively.

In Figure 6.2.1 the frequency response of first experimental trials measuring different tissues are shown and fitted to equation 6.2.4 and the stiffness (k), viscosity (c) and natural frequency (w_n) are determined.
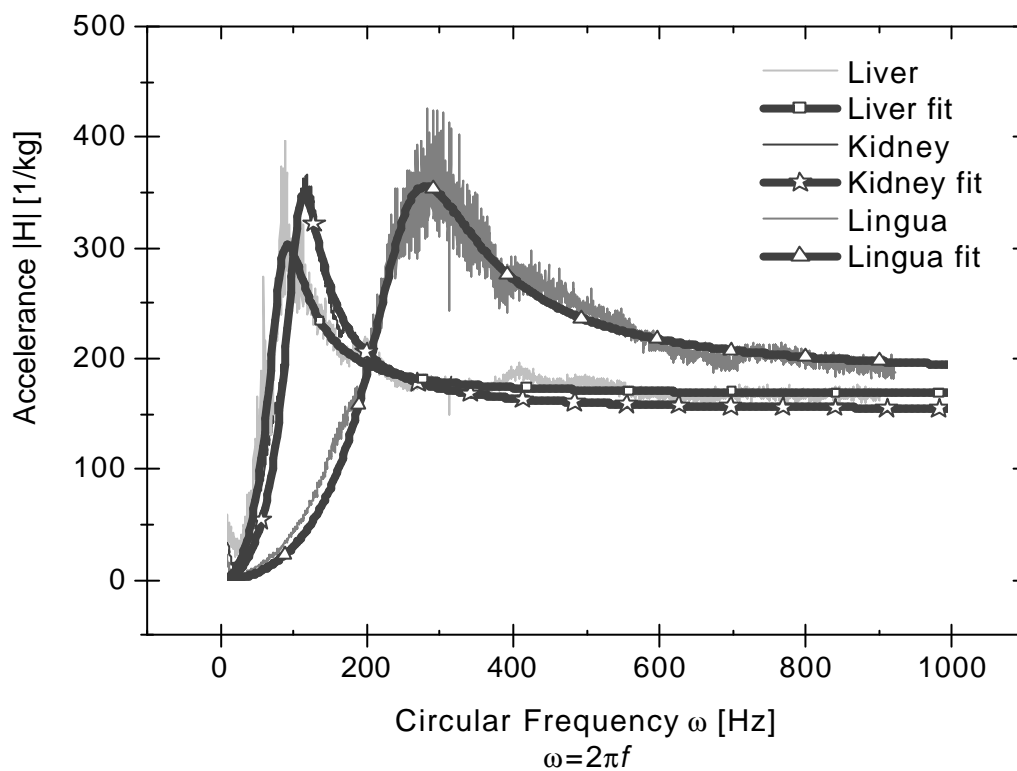

Figure 6.2.1: Frequency Responses of different tissues fitted to the accelerance.

6.3. Modelling the tissue using Multi-Body-Dynamics

Technically, the biological tissue may be modelled as a Multi Degree of Freedom System conveying as many natural frequencies as Degrees of Freedom and delivering the same number of modes. The technical model exists of masses, which are spread out in a three-dimensional grid and dynamically coupled by springs and dampers. When the modal parameters are obtained it should be possible to determine the values of the spring constants and damping values of each link. These results reveal the local

mechanical properties such as elasticity and viscosity that altering throughout one tissue and amongst different types of tissue. Also, it may be possible to recognise the boundary between two neighbouring tissues.

References

[1]   Michal W., *Was den Menschen aufrecht hält,* GEO 2/2004, pp. 98-114 (2004).

[2]   Fletscher T.F., in *Miller's Anatomy of the dog*, eds. H.E. Evans, W.B. Saunders Company Philadelphia, pp. 800-828 (1993).

[3]   MacKinnon P., Morris J. *Lehrbuch der Klinischen Anatomie*, Bern, Hans Huber (1997).

[4]   Panjabi M.M., Goel V. et al. *Spine* **17,** pp. 299-306(1992).

[5]   Mullins L., Effect of stretching on the properties of rubber, J. Rubber Research **16**, pp. 275-289 (1947).

[6]   Mullins L., *Softening of rubber by deformation*, Rubber Chem. Technol. **42**, pp. 339-362 (1969)

[7]   Kohnke P., *Ansys, Inc. theory: release 5.7*, Chapter 4.5, Equation 4.177, Ansys, (2001).

[8]   Rogalla A.R., *Analyse des Spritzgießens mikrostrukturierter Bauteile aus Thermoplasten*, Aachen, Institut für Kunststoffverarbeitung an der RWTH Aachen (1998).

[9]   Tomanek A., *Silicone & Technik Ein Kompendium für Praxis, Lehre und Selbststudium*, München, Wacker-Chemie GmbH (1990).

[10]   Ziegmann C, Wollbold J., *Injection molding process and equipment for molding microscopic plastic components with hollow chambers, undercuts or channel uses soluble plastic insert* Patent Publication number: **DE 19628766**, Applicant: Vereinigung zur Förderung des Institutes für Kunststoffverarbeitung in Industrie und Handwerk an der Rhein.-Westf. Technischen Hochschule Aachen (1998).

[11]   Rosen J., *Force controlled and teleoperated endoscopic grasper for minimally invasive surgery – experimental performance evaluation*, IEEE Transactions on Biomedical Engineering, **46**, pp. 1212–1221 (1999)

[12]   Kühnapfel U., *Endoscopic Surgery Training using Virtual Reality and deformable Tissue Simulation,* Computers & Graphics, **24**, pp. 671-682, (2000)

[13]   Sudhakar M.P. *Modal and Spectrum Analysis: Data Dependent Systems in State Space*, New York, John Willey & Sons, Inc. (1991).

[14]   Ewins D.J. *Modal Testing theory practice and application*, ed. 2, Baldock, England, Research Study Press Ltd. (2000).